Multi-wavelength VLA and Spacecraft Observations of Evolving Coronal Structures Outside Flares

R.F. Willson

Department of Physics and Astronomy, Tufts University, Medford, MA 02155, USA

Abstract. Multi-wavelength Very Large Array (VLA), SOHO and RHESSI observations have been used to study the three- dimensional structure of evolving coronal loops and related signatures of impulsive and long-lasting energy release above active regions. On one day, an enhancement in the 91 cm brightness temperature of an extended coronal loop at the limb coincided with the passage of a coronal mass ejection and EUV ejection event that most-likely originated in an active region behind the limb. We suggest that compression of the corona by the blast wave of the CME produced a global mass redistribution that led to a local increase in the electron density or temperature and a transient increase in the brightness of the 91 cm emission. On another day, an impulsive hard X-ray burst was preceded by gradual changes in the structure of an extended coronal loop connecting the active region to one located on the other side of the solar equator, suggesting pre-burst magnetic evolution at different spatial scales. Changes in the 6 and 20 cm brightness temperature were also detected from the opposite footpoint region suggesting some sort of magnetic connectvity across the solar equator.

---

1. Introduction

Soft X-ray and Extreme Ultraviolet (EUV) images from the Yohkoh, SOHO and TRACE solar missions have been used to study the complex distribution of loops that outlines the large-scale structure of the solar corona within and outside of active regions. These global structures are thought to evolve in response to changes in the underlying magnetic fields or to currents and particle acceleration in the corona.

Radio observations with the Very Large Array (VLA) can extend the results of these orbiting solarmissions by providing complementary information on the size, location, and temporal evolution of coronal loop structures where magnetic energy is stored and released. At 20 and 91 cm wavelength, the VLA can image slowly- varying coronal loops whose emission is produced by the thermal bremsstrahlung of hot coronal plasma trapped in closed magnetic loops anchored to underlying sunspots. Full-disk VLA observations at 91 cm wavelength have revealed large-scale coronal features that can connect distant regions on the Sun (Lang, Willson and Trottet 1988) and VLA observations of simultaneous burst activity at 20 cm wavelength have provided evidence for magnetic loops that can confine and channel energetic particles over large distances (Willson, Lang and Gary 1993).

Here, we discuss recent multi-wavelength observations that combine VLA images (6, 20 and 91 cm) of compact and large-scale coronal loops with SOHO (EIT and LASCO) and RHESSI observations of the transition region and corona. Full-disk VLA maps at 20 and 91 cm together with smaller-field-of-view images at 6 cm wavelength have been used to study the global distribution and evolution of coronal loops at three different heights and the effect that energy release in one part of an active region may have on the structure of the same or distant active region.

2. Observations on 4 July 2001

In Figure 1 we show a VLA snapshot map (1 minute duration) made at 91 cm wavelength on 4 July, 2001 (B configuration) that has been overlaid on a full-disk SOHO EIT image of the Fe XII 195 Å line taken at the same time. The VLA image delineates large-scale (angular extent of $\theta \sim 5'$ - 8'), slowly-varying, coronal loops that extend above and between active regions on the solar disk. The most intense 91 cm emission at the west limb is associated with active region AR9513 whose coronal loop structure is also clearly delineated by EIT. The 91 cm sources have peak brightness temperatures ranging between $T_b = 0.8 - 1.5 \times 10^6$ K, and are most-likely attributed to optically thin thermal bremsstrahlung emission from the corona at a height where the electron density, N_e, is greater than 1.3×10^9 cm^{-3}, the density corresponding to the plasma frequency at 91 cm wavelength. There was no evidence for long-lasting, nonthermal, Type I noise storm emission from any region, as is often observed at 91 cm wavelength (Willson 2000,2002).
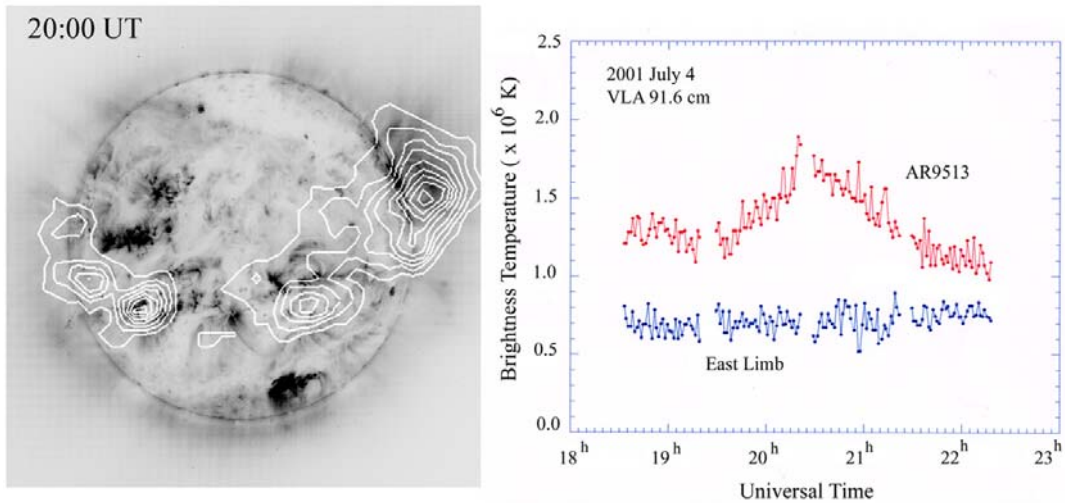
Figure 1. (left) A VLA snapshot map at 91 cm wavelength overlaid on an EIT 195 Å image taken at the same time on 4 July 2001. (right) A plot of the 91 cm brightness temperature from the source associated with AR9513 on the west limb and from the source on the west limb

At ~20:30 UT, the LASCO C2 coronagraph detected a coronal mass ejection (Fig 2) above the northwest limb (position angle P ~34° west of north). The angular width of the CME ~30° and its transverse velocity was estimated to be V ~260 km sec^{-1}. Between 18:00 - 20:00 UT SOHO EIT difference images (Fig. 2) also revealed filamentary EUV emission moving outward along an arc through the middle corona at about the same position angle as the CME This emission is possibly associated with an erupting filament during the onset of the CME that was later seen by the LASCO C2 coronagraph. The source region of this EUV-emitting plasma is uncertain, but it likely originated within an active region behind the northwest limb, as its trajectory lies clearly north of the limb region AR9513.
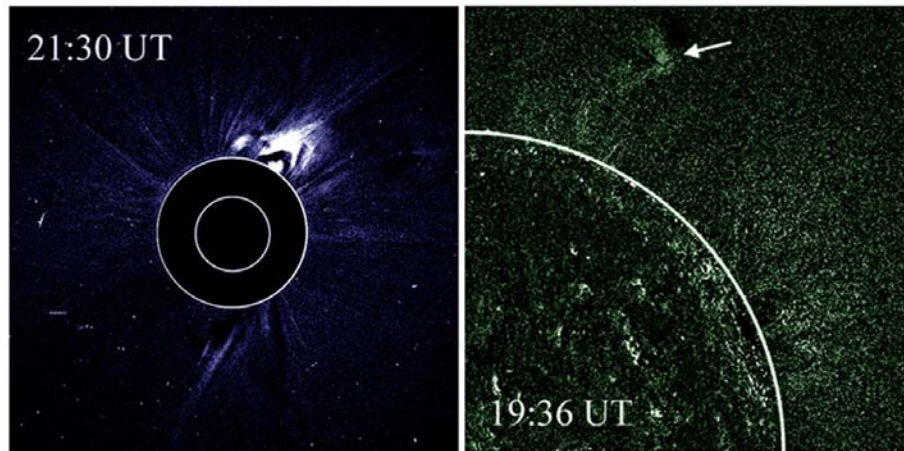
Figure 2. A LASCO C2 coronagraph image (left) and an EIT 195 Å image (right) showing the development of a CME and EUV ejection event on 4 July 2001.

   Although the 91 cm emission on the west limb does not extend as far north as the region where the ascending EUV emission was detected, Figure 1 shows that the peak brightness temperature of the 91 cm source increased from $T_b \sim 1.2 \times 10^6$ K to $\sim 1.8 \times 10^6$ K between 19:30 - 20:30 UT; it then gradually decreased to its baseline level over the next 1.5 hours, or approximately when the CME was detected above $2R_o$ by LASCO. VLA snapshot maps also show that the centroid of the 91 cm emission moved about 1'-2' southward over this time period. There was no evidence for impulsive, Type III burst 91 cm emission at any time, as has been detected during some CMEs (eg. Gopalswamy et al;. 1999; Pohjolainen et al. 2001). Similarly, examination of the EIT images showed no significant changes in the brightness or structure of the EUV loops associated with AR9513, as might be expected from flare-initiated heating or magnetic changes of the coronal loop plasma. We therefore suggest that large-scale restructuring and/or compression of the corona by the blast wave of the distant CME led to an increase in the electron temperature or density in this region. This would increase the optical depth and brightness of both thermal bremsstrahlung and nonthermal plasma emission from the source, but in the absence of detailed spectral information, we cannot distinguish between these two radiation mechanisms. For example, if the emission mechanism is assumed to be thermal bremsstrahlung, then the observed increase in brightness temperature could be explained if the electron density increased by a factor of ~1.6. The signatures of global compression, mass redistribution and restructuring of complex magnetic systems by the shock waves of passing CMEs has also been suggested by EUV "dimming" of the chromosphere and corona (so-called EIT waves -Thompson et al. 1999) and by the appearance of nonthermal radio sources located far from the sites of CMEs (Maia et al. 1999).

3. Observations on 30 March 2003

   On 2003 March 30, the VLA (C configuration) detected bright ($T_b = 2$-3.2×10^6 K), unpolarized ($\rho_c < 10\%$) emission at 20 cm wavelength from active regions AR0321 (N04 E11) and AR0323 (S08 W01) and from the trans-equatorial region between them (Fig. 3). Bright emission at 6.2 cm wavelength from the target region AR0323 was also detected; reliable images at 6.2 cm were not obtained for AR0321, located 5' to the northeast, because this active region was outside of the half-power point of the VLA primary beam.

   VLA snapshot maps (1-minute intervals) at 20.7 cm indicate that these sources underwent significant changes in brightness temperature over the five hour period of observation. As illustrated in Figure 3, the peak brightness temperature of AR0323 began to increase from $T_b \sim 2 \times 10^6$ K ~17:00 UT and reached a maximum of $T_b = 3.2 \times 10^6$ K about an hour later. It then

declined steadily to about $T_b = 1.5 \times 10^6$ K by 20:00 UT. In contrast, the peak brightness temperature of AR0321 began to decline steadily from a peak of $T_b = 2.7 \times 10^6$ K at ~16:40 UT to $T_b = 1.8 \times 10^6$ K at 18:30 UT followed by a small increase over the next hour.
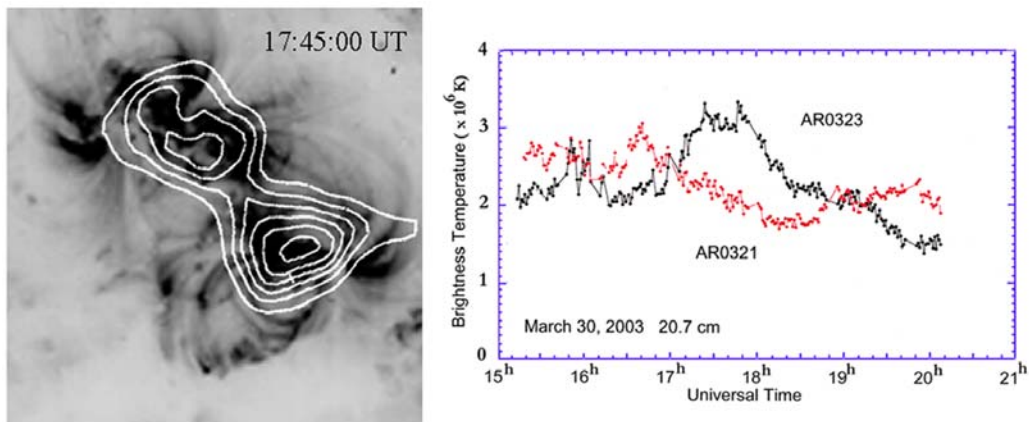
Fig ure 3. (left)VLA snapshot maps at 20.7 and 6.2 cm (inset) wavelength at 17:36 UT are overlaid on a SOHO MDI photospheric magnetogram taken at about the same time. (right) A plot of the peak 20.7 cm brightness temperature from active regions AR0321 and AR0323.}

These 20 cm wavelength variations were accompanied by hard X-ray burst emission from AR0321 (RHESSI) and by changes in the structure of the Fe XII 195 Å EUV loop emission (SOHO EIT) in the equatorial region between the two active regions. As shown in Figure 4, a relatively weak "precursor" burst was detected by RHESSI at 17:35 UT, followed by a significantly larger event at 17:44 UT. The main hard X-ray burst was followed a C1.3-class GOES soft X-ray burst at 17:47 UT. RHESSI snapshot maps in the energy range between 6-12 keV (Fig 4) indicate that the burst and its precursor originated at the same location within AR0321. The impulsive hard X-ray bursts were then followed by more slowly-varying changes in the EUV emission detected in the trans-equatorial region between AR0321 and AR0323. As can be seen in the series of EIT images shown in Figure 5, the diamond-shaped area of low-brightness EUV emission along the southeastern edge of AR0321 began to extend westward along the solar equator starting at $\approx$18:00 UT. This evolving EUV source probably delineates plasma at a higher or lower temperature than that outlined by the Fe XII emission which has a peak formation temperature of T ~1.5 x 10^6 K. This moving plasma might then be attributed to flare ejecta from the hard X-ray burst or to heating of the coronal loops in this region. We note that the intensity of the 20 cm loop in the trans-equatorial region overlying the evolving EUV emission decreased in intensity during this period, probably in response to the changing electron temperature, density, or both.
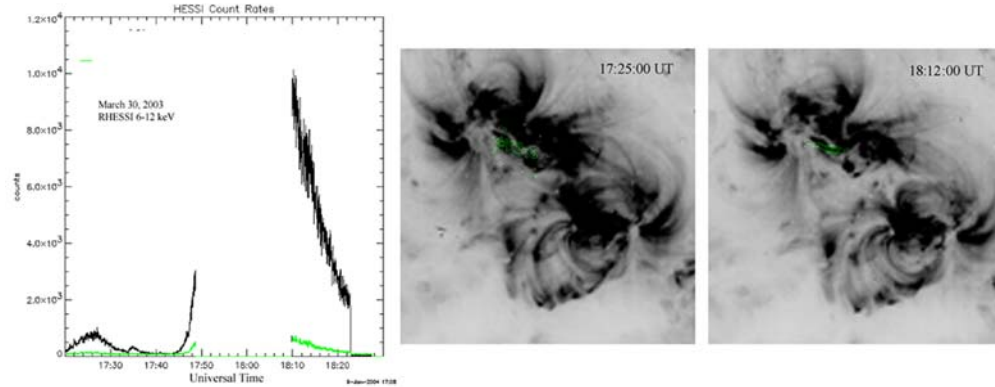
Figure 4. (left) Time profile of the RHESSI count rate in the energy range between 6.2 - 9.2 keV and 9.2 -12.3 keV showing the hard X-ray burst emission between 17:25-18:25 UT. (right) RHESSI snapshot images (20 sec intervals) are overlaid on SOHO EIT 195 Å images of AR0321 at the times indicated. Here, the field-of-view is 10' x 10'

As shown in Figure 6, the 6 cm emission from AR0323 also varied significantly during this time period. The 6 cm emission consists of two main sources (W and E) with a fainter bridge of emission connecting them. These sources overly the leading and trailing sunspots of negative and positive magnetic polarity, respectively, while the narrower bridge overlies a more compact area of predominantly negative polarity near the center of the active region. These evolving 6 cm sources are most-likely attributed to thermal gyroresonance emission at the second or third harmonic, s, of the gyrofrequency; they therefore outline coronal plasma where the magnetic field strength has a value of B = 857 G (s = 2) or B = 570 G (s = 3). Examination of a series of MDI magnetograms (Fig 6.) show the growth and migration of a number of small magnetic elements (arrows) between the sunspots during the period of the VLA observations

Snapshot maps at both 6 and 20 cm wavelength as well as images from RHESSI showed no evidence for low-level impulsive bursts from AR0323 as might be expected if these evolving magnetic fields induced electric currents and triggered magnetic reconnection events and the production of energetic particles whose impulsive gyrosynchrotron emission could be detected at radio wavelengths. We therefore suspect that the changes in brightness temperature shown in Figures 3 and 6 are related to slower resistive heating of the coronal plasma in response to these evolving photospheric magnetic fields.
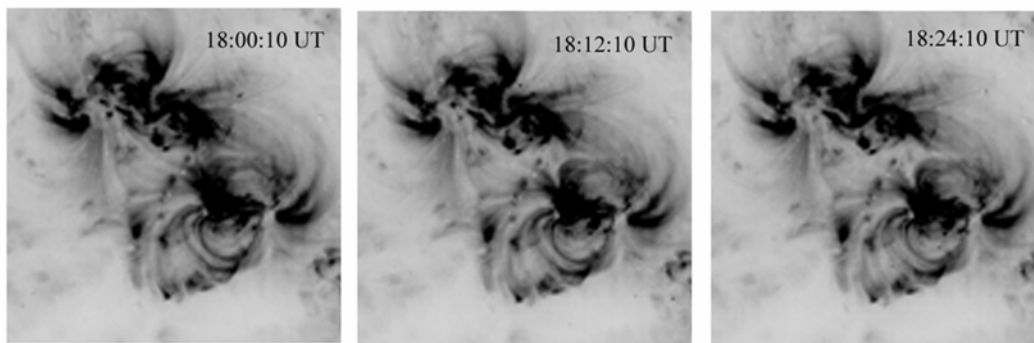
Figure 5. A series of SOHO EIT 195 Å images showing the temporal evolution of the EUV emission from AR0321, AR0323 and the trans-equatorial region between them. Here, the gray-scale levels of the image have been inverted to provide better clarity.
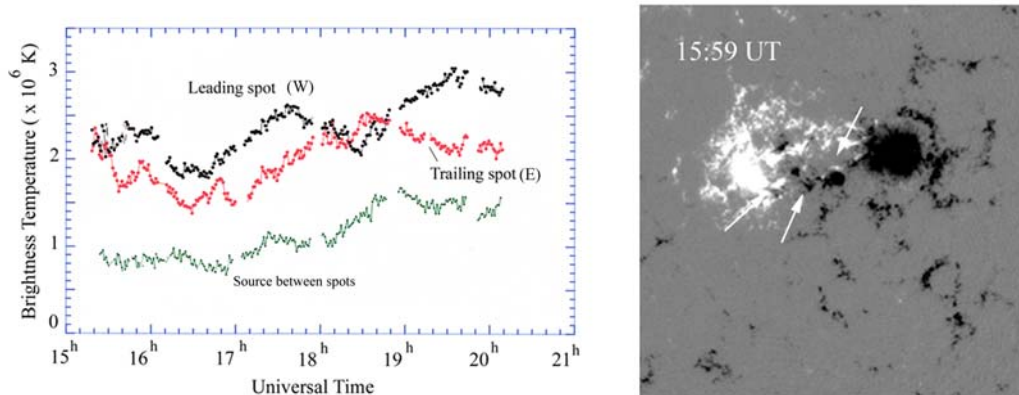
Figure 6. (left) Time profiles of the peak brightness temperature at 6 cm wavelength from the two sunspot-associated components within AR0323 and the source between them. (right). A series of MDI magnetograms of AR0323 at the times indicated. Here, the field-of-view is 4' x 4'. The arrows mark the location of emerging and evolving patches of magnetic flux that may be related to the evolving 6 and 20 cm emission from this region.

4. Summary and Conclusions

Our multiwavelength VLA, SOHO and RHESSI observations have shown that the complex coronal environment above active regions may be influenced by energy release or magnetic reconfiguration initiated outside the active regions. On 4 July 2001, we find evidence that the thermal environment of the corona above a relatively quiescent active region may have been perturbed and compressed by the blast wave of a CME originating behind the limb. This led to global changes in the electron density or electron temperature, and to a transient increase in the 91 cm brightness temperature of the region on the visible solar disk. On 30 March 2003, slowly-evolving 20 cm emission associated with coronal loops joining sunspots of opposite magnetic polarity in the same active region as well as in large-scale trans-equatorial loops joining the two regions was observed during times of impulsive and slow energy release. The evolving 20 cm loops may have been part of a more extensive magnetic reconfiguration involving impulsive hard X-ray bursts in one region and slow magnetic heating in the other. As described by Uchida et al (1992) slow expansion of anti-parallel magnetic fields in the two active regions may drive magnetic reconnection and supply flux to a reconnection site at the equator, leading to the formation of the trans-equatorial loops themselves.

References

Gopalswamy, N. et al. 1998 *J. Geophys. Res.* 103, 307.
Lang, K.R., Willson R.F., \& Trottet 1988, *Astron. \& Astrophys.* 199, 325.
Maia, D., Pick, M., Vourlidas, A., & Howard, R.} 2000, *J. Geophys, Res.* 105, 18215.
Pohjolainen, S., et al. 2001, *Ap. J.* 556, 421.
Thompson, B.J., Gurman, J.B., &Neupert, W.M. et al 1999, *Ap. J. (Letters)* 517. L151.
Uchida, Y. et al} 1992, Pub. *Astron. Soc. Japan* 44. L55.
Willson, R.F., 2000, *Solar Phy* 197, 399.
Willson, R.F., 2002, *Solar Phy.* 211}, 289.
Willson, R.F., Lang, K.R., \& Gary, D. 1993 *Ap.J.* 418, 490.